

# Linear Low-Density Polyethylene Formulated with Photoluminescent Additive for Rotational Molding

Carlos A. Téllez<sup>a\*</sup>, Helia B. Leon-Molina<sup>b</sup>

<sup>a</sup>Producciones Generales S.A, Cr 3 # 56-07 Soacha, Colombia.

<sup>b</sup>Universidad ECCI, School of engineering, Materials and Processes Master's Program, Mailing address: Cl. 51 # 19-12 Bogotá, Colombia. [id.manufactura01@progen.com.co](mailto:id.manufactura01@progen.com.co)

This work studies the properties of Linear Low-Density Polyethylene (LLDPE) doped with strontium aluminate at concentrations of 3% and 15% m/m with possible applications in road safety products manufactured by rotational molding. To this aim, the design and manufacture of a prototype part and the mold for the rotational molding process were carried out. Single-layer parts as well as bilayer parts were manufactured, subsequently, samples of the obtained pieces were subjected to Fourier Transform Infrared Spectrometry (FTIR), Scanning Electron Microscopy (SEM), X-ray Diffraction Analysis (XRD), UV-VIS spectrometry and photoluminescence measurements. The mono-layer and bilayer samples with 15% m/m of strontium aluminate showed the highest decay luminescence times -between 81 h and 92 h-. In the UV-vis fluorescence test, the bilayer piece with 15% m/m of additive showed the highest absorption intensity during the excitation process. The SEM images showed the external surface and the cross section of samples. In conclusion, the rotomolded LLDPE with 15% w/w of strontium aluminate doping could be used as a photoluminescent material for road safety products.

## 1. Introduction

Smart highways are currently being designed, which will require efficient, low-cost, signaling methods (Avenidaño, 2014). A specific need on this regard has been identified in Spain, as lighting highways, even with a low consumption system, is totally unfeasible due to the high costs that this represents (Villareal, 2014). Based on this background, the company PROGEN S.A, which is aimed to manufacture rotomolded parts, has identified the need to produce road marking parts for low visibility environments, as an alternative to similar parts that are used nowadays, by complementing them with reflectors, reflective tapes, and painting. This entails cost overruns for the initial rotomolded part (Tonikian et al., 2006). Therefore, new photoluminescent materials have been developed, such as photoluminescent compounds of frequently used based on polymeric matrices, i.e., polyethylene (PE). This would make traffic signals and road indications visible through the use of unconventional energy sources, such as sunlight or an alternative light source. Hence, this research analyzes a photoluminescent material linked to a low-cost process and production of large-volume parts such as rotational molding. Likewise, it has been possible to obtain products with photoluminescent optical characteristics in other transformation processes of thermoplastic materials, which show sufficient emission in long ranges of time (Saito and Yamamoto, 2000). The purpose of this work is to obtain a linear low-density polyethylene formulation with a photoluminescent additive, which can be processed through rotational molding in order to obtain a final piece with road marking applications.

## 2. Materials and methods

In order to achieve the stated objectives, the following stages were carried out: proposal of the polymer and photoluminescent additive formulations, design of the rotational molded prototype piece, design and manufacture of the required rotational mold for the manufacture of the pieces, and finally, the characterization of the formulations. The materials, equipment, and procedures used in each stage are described below.

## 2.1 Formulation proposal

The photoluminescent formulations were prepared using Linear Low-Density Polyethylene (LLDPE) RO93650 NAT from POLIMEROS NACIONALES S.A. DE C.V as polymeric material and strontium aluminate doped with europium and dysprosium (SrAl<sub>2</sub>O<sub>4</sub>: Eu<sup>+2</sup>, Dy<sup>+2</sup>) reference YG-D4Z from JOLIN CORPORATION as the photoluminescent additive (PA). The composition of the prepared formulations is shown in Table 1.

Table 1: Composition of LDPE/

Formulation	LDPE (% w/w)	PA (%w/w)
PE	100	
PEPA15	85	15
PEPA3	97	3

The nomenclature of the formulations consists of the abbreviations of the components and a number indicating the percentage of photoluminescent additive content. In this way, the PEPA15 formulation is made up of 85% LLDPE and 15% photoluminescent additive.

## 2.2 Design of the Prototype Piece and the Rotational Molding Mold for its Manufacture.

The criteria of geometry and shape for polymer material parts manufactured through the rotational molding process were used for the design of the prototype pieces. Considering the geometry of the piece that was designed, the mold for rotational molding was designed, which consists of a uniform thickness cavity of 2.0 mm. The 3D models of the design and the manufacturing plans of the piece and the mold were made using the SolidEdge program, version 2021.

## 2.3 Mold and Prototype Piece Manufacturing

The cavity was manufactured using 6061 Aluminum, supplied by Dimecol Ltda, with a thermal conductivity of 0.217 kW/m\*K at 20°C. On the other hand, the tools required for the mold anchoring were made using A-36 Steel from the supplier GandJ. The manufactured mold was coupled to the ROTOLINE brand Shuttle rotational molding machine, Model DC-2.50. The production of the pieces was carried out using two processing methodologies that determined the distribution of the additive in the piece: single-layer and bi-layer. Single-layer: all the mixture was added to the mold in one step. Bi-layer: the piece is formed in two stages, in the first one, 50% of the polymer with the entire additive is added to the mold, in the second one, the remaining polymer is added. The process parameters are shown in Table 2.

Table 2: Process parameters

Parameter	Bi-layer process 1	Bi-layer process 2	Single-layer process	Cooling
Temperature (°C)	250	250	250	-
Time (min)	6	6	12	9
Primary speed (rpm)	4.0	4.0	4.0	1.0
Secondary Speed (rpm)	1.5	1.5	1.5	1.0

## 2.4 Characterization of the formulations

Samples of the rotomolded prototype pieces were subjected to optical, chemical, and morphological characterization. The conditions used for the different characterization tests are explained below. **UV-vis fluorescence spectroscopy:** The Spectronic brand spectrophotometer, reference Genesys 2Pc, was used with a scan between 340 nm and 700 nm, at a speed of six points per nanometer in absorbance mode. **Luminance:** It was carried out through a Minolta brand luminance meter, reference LS-100, which was configured in units of Cd/m<sup>2</sup> and absolute measurement values, based on the parameters of the UNE 23035-12003 standard, and a 30 W UV light source, uvBEAST brand reference V3, wavelength (λ) between 385-395 nm. The samples were isolated 24 hours before the test was carried out in a completely light-free environment, and then stimulated with the light source for 5 minutes for each of the samples, and then measurements were taken at 5-minute intervals up to 120 minutes. The attenuation times were defined through the extrapolation of the graph until a value of 0.32 mcd/m<sup>2</sup> was achieved as indicated in the corresponding standard. **Morphology:** Optical and Scanning Electron Microscopy (SEM) was performed of the surface and cross section of the samples were performed. A digital Dino-Lite microscope, reference AM3111, with 19x amplification was used for optical microscopy. SEM photographs were taken on a JEOL JCM-5000/Neoscope Scanning Electron Microscope, with a 5 kV EHT current, 50x amplification, and a secondary electron detector. The SEM samples were prepared with a gold coating using a Creisington sputter coater 108 auto equipment. **Chemical Characterization (FTIR):** The Alpha Sample Compartment RT-DLaTGS spectrophotometer from Bruker Optik GmbH was used for the test, performing 32 scans in times ranging from 2 to 5 minutes, correcting for the

presence of carbon dioxide, humidity or water. **Structure (DRX):** The X-ray diffraction (XRD) analyses were performed using an X'pert Pro Panalytical diffractometer, using an empyrean cobalt tube ( $\lambda = 1.7889 \text{ \AA}$ ), with a scan speed of 0.5 seconds per step in a  $2\theta$  range between  $10^\circ$  and  $90^\circ$ . Data analysis was performed using the OriginPro software.

### 3. Results

#### 3.1 Prototype piece and roto-molding mold design and manufacture

Figure 1 (A) shows the prototype piece design layout to verify the performance of the LLDPE and strontium aluminate formulations in the rotational molding process. The smoothing of the geometry to allow the flow of the material, along with the staggered surfaces to give reinforcement and rigidity to the piece can be observed, as well as the use of uniform thicknesses of 2 mm in order to eliminate possible deformations of the final piece due to differential contractions. In addition, draft angles with a subtraction zone that facilitated the removal of the piece from the mold were considered. Figure 1 (B) shows a schematic of the roto-molding mold that was designed and manufactured in order to obtain the prototype pieces, and Figure 1 (C) shows the luminescent appearance of the manufactured pieces.

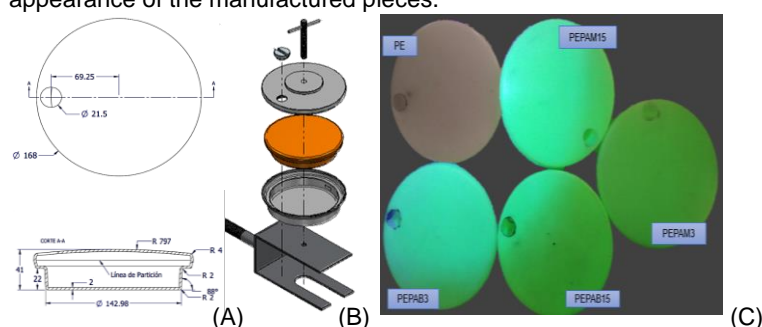


Figure 1. Prototype piece and roto-molding mold. (A) Plan of the prototype piece. (B) Scheme of the designed mold. (C) Prototype piece manufactured by rotational molding.

#### 3.2 Optical Characterization. UV-vis spectrometry and Luminance measurement

The Figure 2 (A) and (B) shows the results of energy absorbance and luminance attenuation from the samples respectively. As it can be observed in Figure 2 (A), the PE sample shows a single peak around 346 nm with a subsequent continuous decay. On the other hand, all samples with luminescent additive content show multiple peaks, the first one around 353 nm.

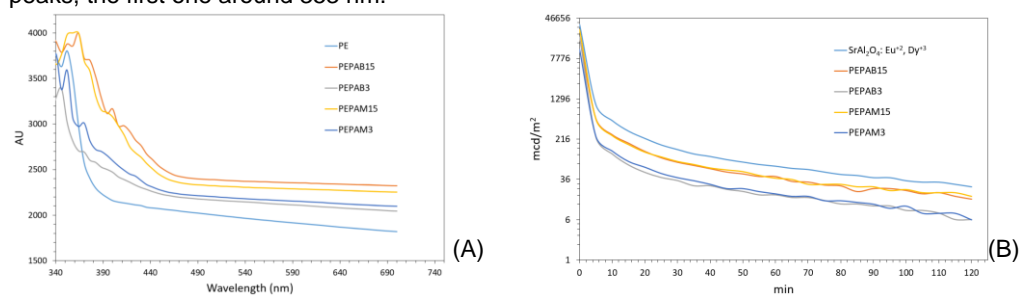


Figure 2: Optical characterization results. (A) UV-Vis samples spectrum absorbance. (B) Photoluminescence lifetime.

The PEPAB3 and PEPAM3 samples show a lower intensity peak of around 370 nm followed by a continuous decay. Additionally, it is observed that among the samples with 3% w/w of additive, the PEPAM3 formulation shows an intensity from 2% to 5%, which is higher than the PEPAB3 sample throughout the whole wavelength range that is being studied. On the other hand, the PEPAB15 and PEPAM15 samples have a similar absorption pattern, and surpass in absorption intensity those samples with 3% of additive and those with the natural polymer. Thus, they show the highest absorption rate: around 364 nm, and local maxima around 376 nm, 400 nm, and 412 nm. Previous studies found absorption peaks between 306 to 359 nm (Chitnis et al., 2019) and around 390 nm (Khurshheed et al., 2018). Finally, Khattab found an energetic absorption peak around 366 nm (Khattab et al., 2019). The results of the luminance attenuation measurement that was performed on samples:

PEPAB3, PEPAM3 PEPAB15, PEPAM15, and pure strontium aluminate are displayed in Figure 2 (B). As expected, pure strontium aluminate showed higher luminance than the formulations with 3% m/m and 15% m/m of this additive. These results show an average reduction of 41% and 73% in the samples luminance with 15% and 3% of additive, respectively. Table 2 shows the decay time until reaching a luminance value of 0.32 mcd/m<sup>2</sup>, which is the minimum viewing value according to the UNE 23035-12003 standard.

Table 3: Data extrapolation to achieve a luminescence of 0.32 mcd/m<sup>2</sup>

Sample	Average attenuation time (min)	Error %	% Diff.
SrAl <sub>2</sub> O <sub>4</sub> : Eu <sup>+2</sup> , Dy <sup>+3</sup>	6397.75	0.04	-
PEPAB15	4857.51	0.04	24 %
PEPAB3	2474.52	0.02	61 %
PEPAM15	5517.84	0.03	14 %
PEPAM3	2303.25	0.02	64 %

It was observed that the minimum attenuation time under the influence of the light source in the UV range corresponded to sample PEPAM3, which was 38 hours of continuous light emission. The results obtained with samples PEPAM15 and PEPAB15 are to be highlighted, revealing attenuation times of 91 hours and 81 hours, respectively. Regarding the percentage difference compared to pure strontium aluminate, it was observed that samples PEPAM15, PEPAB15, PEPAB3, and PEPAM3 showed an attenuation time reduction of 14%, 24%, 61%, and 64%, respectively. The non-linear decay behavior observed in this study is similar to that obtained by Khattab et al., 2019, which also has a similar profile to that found by Jiang et al., 2014, as well as Saito and Yamamoto, 2000, who carried out fluorescence decay analyses on various types of photoluminescent compounds. An ANOVA type analysis was performed on the luminance values obtained at 60 min. It showed that the variable with the highest effect on this property is the additive concentration that was used on the samples.

### 3.3 Light Microscopy and SEM

Figure 3 shows the surface and cross sections of the samples through optical micrographs. It is evident that the PE sample does not show luminescence, on the contrary to what was observed with the samples that were formulated with the additive, PEPAM15, PEPAB15, PEPAB3, and PEPAM3.

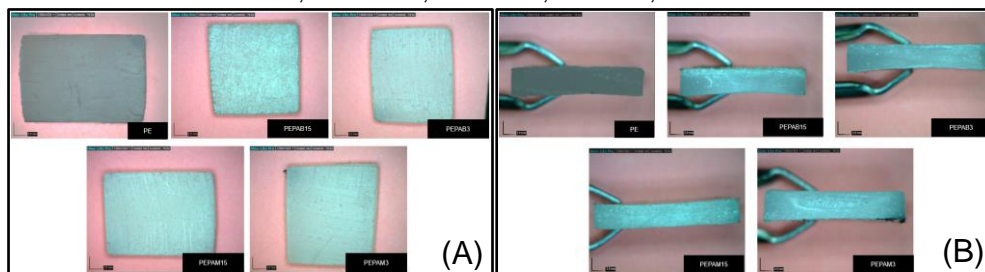


Figure 3: Photographs of the samples at 19x: (A) External surface, (B) Cross section

On the one hand, in figure 3 (B), it is observed that in the cross section of the PEPAM15 and PEPAM3 samples, a uniform distribution of the additive through the thickness is evident, this is due to the fact that, in the single-layer manufacturing process, the additive is all mixed with the polymer in the matrix. On the other hand, the PEPAB15 and PEPAB3 formulations show higher photoluminescence on the surface of the sample, which may be due to the bilayer manufacturing methodology that was used. It consisted on the external layer containing all the photoluminescent additive. Figure 4 shows more detail of the samples' surface and cross section that are studied, through the SEM technique. In Figure 4 (A), surface porosities are evident in all the study pieces, which may be related to the particle sizes of the polymeric matrix used for the roto-molding process (Baumer et al., 2014) and to the presence of particulate additives in the formulation in the case of samples PEPAM15, PEPAB15, PEPAB3, and PEPAM3.

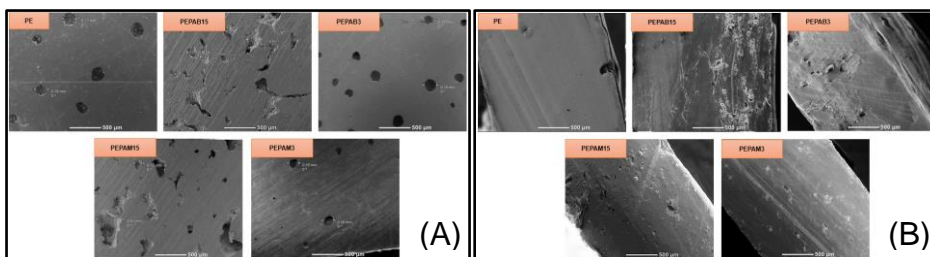


Figure 4: SEM images of the samples with 50x magnification: (A) External Surface, (B) Cross section

However, a change in the geometry of the porosities cross section from quasi-circular to irregular is observed, as well as porosities increase, by increasing the additive concentration. Previous studies have shown the direct proportional relationship between the appearance of porosities in mixtures and the increase in the concentration of added particulate additive (Shaker and Rodrigue, 2019).

### 3.4 X-ray diffraction and Infrared Spectroscopy

In Figure 5 are shown the X-ray diffractograms and the FTIR spectra of formulations. In Figure 5 (A), the results for PE sample, the typical peaks for polyethylene are observed at  $26^\circ$  and  $29^\circ$  corresponding to the crystalline planes (110) and (200) respectively, of the orthorhombic polyethylene unit cell (Alsaygh et al., 2014). Furthermore, a decrease in the peaks' intensity is observed with the content increase in the luminescent additive mix. This effect is more notorious for the PEPAB15 sample, in which, in addition to the total disappearance of the  $29^\circ$  peak, a slight shift of the peak that was initially at  $26^\circ$  is also observed. This may be due to a change in the polyethylene network parameter due to the presence of the additive in the polymeric matrix. Similar effects of typical XRD peak shifts for a polymeric matrix have also been observed before. For instance, Poulouse et al., in 2021, detected a shift in the typical peaks for polypropylene (PP) crystals in the presence of a photoluminescent additive (Poulouse et al., 2021). Benabid et al. mixed high-density polyethylene (HDPE) with zinc oxide (ZnO). They found a peaks reduction of the polymer that was used, probably due to the presence of the added ceramic material (Benabid et al., 2019). Finally, Bem et al. in 2009 detected an intensity decrease of the XRD peaks of low-density polyethylene (LDPE) in the presence of strontium aluminate (Bem et al., 2009).

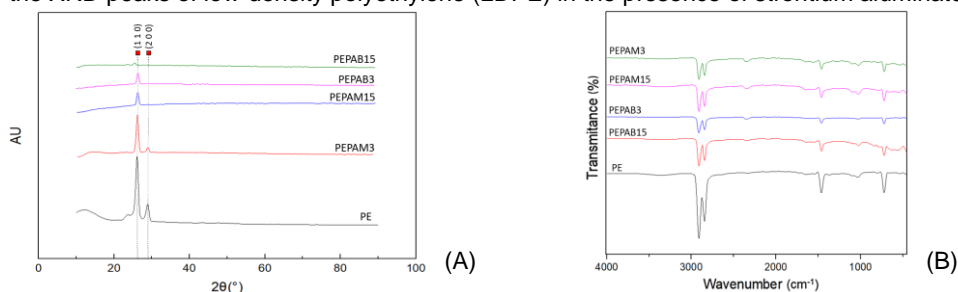


Figure 5: (A) XRD samples pattern. (B) IR spectrum of the samples

Figure 5 (B) shows the FTIR spectra obtained for the PEPAM15, PEPAB15, PEPAB3, and PEPAM3 samples. The spectrum corresponding to the sample that was identified as PE, as it was expected, shows the typical peaks for linear low-density polyethylene, highlighting the peaks corresponding to stretching, deformation, and C-H bond shaking vibrations at wavelengths between  $2830\text{ cm}^{-1}$  and  $2950\text{ cm}^{-1}$ ,  $1460\text{ cm}^{-1}$  and  $720\text{ cm}^{-1}$ , respectively (Zhao et al., 2018). It should be highlighted that the spectra obtained from the formulations with strontium aluminate content showed peaks located at the same wavelengths, with the same shape. This behavior is possible evidence of the chemical interactions' absence between the LDPE polymeric matrix and the photoluminescent additive. Similar results were obtained by Prakash et al., 2018 and Lin et al., 2012.

## 4. Conclusions

Formulations at 3 % m/m and 15 % m/m of strontium aluminate doped with europium and dysprosium in LLDPE matrix were used to fabricate single layer and bilayer rotomolded complete parts with uniform thicknesses. The results of the characterization tests that were carried out did not allow drawing a conclusion about the possibility of chemical interactions between the polymer and the additive. Specifically, the X-ray diffraction results indicate a possible change in the polymer lattice parameter with increasing photoluminescent additive content, while the

location invariance of the infrared spectrum peaks are an indication of the absence of interactions among the polymer and the additive. The 15% m/m formulation of strontium aluminate that was manufactured with the monolayer methodology (PEPAM15) is recommended by means of it showed the best efficiency between formulation and manufacturing costs with luminance results.

### Acknowledgments

The authors acknowledge the company PROGEN S.A for funding this project and the ECCI University for supporting the FTIR tests and gold coatings for the pieces that were tested.

### References

- Alsaygh A. A., Al-Hamidi J., Fares Alsewailam D., Al-Najjar I. M., Kuznetsov V. L. 2014. Characterization of polyethylene synthesized by zirconium single site catalysts. *Applied Petrochemical Research* 2014 4:1, 4(1), 79–84. <https://doi.org/10.1007/S13203-014-0053-2>
- Avendaño G. 2014. *Se prueba la pintura fluorescente para mejorar la visibilidad en las carreteras | Motor*. <https://www.motor.com.co/actualidad/prueba-pintura-fluorescente-mejorar-visibilidad-carreteras/18025>
- Baumer M. I., Leite J. L., Becker D. 2014. Influence of calcium carbonate and slip agent addition on linear medium density polyethylene processed by rotational molding. *Materials Research*, 17(1), 130–137. <https://doi.org/10.1590/S1516-14392013005000159>
- Bem D. B., Luyt A. S., Dejene F. B., Botha J. R., Swart H. C. 2009. Structural, luminescent and thermal properties of blue SrAl<sub>2</sub>O<sub>4</sub>:Eu<sup>2+</sup>, Dy<sup>3+</sup> phosphor filled low-density polyethylene composites. *Physica B: Condensed Matter*, 404(22), 4504–4508. <https://doi.org/10.1016/j.physb.2009.09.050>
- Benabid F. Z., Kharchi N., Zouai F., Mourad A. H. I., Benachour D. 2019. Impact of co-mixing technique and surface modification of ZnO nanoparticles using stearic acid on their dispersion into HDPE to produce HDPE/ZnO nanocomposites. *Polymers and Polymer Composites*, 27(7), 389–399. <https://doi.org/10.1177/0967391119847353>
- Chitnis D., Thejo Kalyani N., Dhoble S. J. 2019. Comprehensive study on photophysical properties of Eu(TTA) 3 bipy phosphor molecularly doped in PMMA and PS matrices. *Results in Physics*, 13, 102302. <https://doi.org/10.1016/j.rinp.2019.102302>
- Jiang T., Wang H., Xing M., Fu Y., Peng Y., Luo, X. 2014. Luminescence decay evaluation of long-afterglow phosphors. *Physica B: Condensed Matter*, 450, 94–98. <https://doi.org/10.1016/j.physb.2014.04.080>
- Khattab T. A., Abd El-Aziz M., Abdelrahman M. S., El-Zawahry M., Kamel S. 2019. Development of long-persistent photoluminescent epoxy resin immobilized with europium (II)-doped strontium aluminate. *Luminescence*. <https://doi.org/10.1002/bio.3752>
- Khursheed S., Sheergojri G., Proceedings J. S.-M. T., 2018. Phosphor Polymer Nanocomposite: SrAl<sub>2</sub>O<sub>4</sub>:Eu<sup>2+</sup>, Dy<sup>3+</sup> Embedded PMMA for Solid-State Applications. *Materials Today. Connecting the Materials Community*, 2096–2104. <https://www.sciencedirect.com/science/article/pii/S2214785320304284>
- Lin H., Chen B., Chen Y., Chen G., Lin H., Zheng Z., Chen Z., Guo H., Huang L., Chen, Z. 2012. Encapsulation of polyethylene for strontium aluminate phosphors to enhance its water resistance. *Advanced Materials Research*, 393–395, 84–87. <https://doi.org/10.4028/www.scientific.net/AMR.393-395.84>
- Poulose A. M., Anis A., Shaikh H., Alhamidi A., Kumar N. S., Elnour A. Y., Al-zahrani S. M. 2021. Strontium Aluminate-Based Long Afterglow PP Composites: Phosphorescence, Thermal, and Mechanical Characteristics. *Polymers* 2021, Vol. 13, Page 1373, 13(9), 1373. <https://doi.org/10.3390/POLYM13091373>
- Prakash J., Kumar V., Erasmus L. J. B., Duvenhage M. M., Sathiyam G., Bellucci S., Sun S., Swart H. C. 2018. Phosphor Polymer Nanocomposite: ZnO:Tb<sup>3+</sup> Embedded Polystyrene Nanocomposite Thin Films for Solid-State Lighting Applications. *ACS Applied Nano Materials*, 1(2), 977–988. <https://doi.org/10.1021/acsnm.7b00387>
- Saito M., Yamamoto K. 2000. Bright afterglow illuminator made of phosphorescent material and fluorescent fibers. *Applied Optics*, 39(24), 4366. <https://doi.org/10.1364/ao.39.004366>
- Shaker R., Rodrigue, D. 2019. Rotomolding of Thermoplastic Elastomers Based on Low-Density Polyethylene and Recycled Natural Rubber. *Applied Sciences*, 9(24), 5430. <https://doi.org/10.3390/app9245430>
- Tonikian R., Proulx G., Bénichou N., Reid I. 2006. LITERATURE REVIEW ON PHOTOLUMINESCENT MATERIAL USED AS A SAFETY WAYGUIDANCE SYSTEM Literature Review on PLM. In *everglow.us*. <http://www.everglow.us/pdf/nrc-literature-review-of-pl-path-marking-march-2006-rr-214.pdf>
- Villareal D. 2014. *Así funciona la carretera del futuro y sus líneas fosforescentes | Diariomotor*.
- Zhao P., Lu C., Gao X. P., Yao D. H., Cao C. L., Luo Y. J. 2018. Regulating the Microstructure of Intumescent Flame-Retardant Linear Low-Density Polyethylene/Nylon Six Blends for Simultaneously Improving the Flame Retardancy, Mechanical Properties, and Water Resistance. *ACS Omega*, 3(6), 6962–6970. <https://doi.org/10.1021/ACSOMEGA.8B00488>